INFLUENCE OF Sn AND Al HETEROATOMS ON THE SYNTHESIS OF ILERITE

Wojciech Supronowicz* and Frank Roessner

Carl von Ossietzky University, Faculty of Natural Sciences, Industrial Chemistry II, D-26-111 Oldenburg, Germany

Abstract—Hydrothermal syntheses of a silicate structure comprising a single tetrahedral layer, known as ilerite, were conducted in the presence of tin ($SnCl_4 \cdot 5H_2O$) as a heteroatom. The main aim of the study was to investigate the influence of the above-mentioned compound on the resulting material, as well as the possibility of isomorphous replacement of Si by Sn atoms. For comparison, unmodified ilerite, ilerite impregnated by SnO_2, and ilerite synthesized in the presence of Al (aluminum isopropoxide) were also used. The ilerite structure observed was that of Na-ilerite. Syntheses of samples with various Sn/Si ratios (up to the value of 0.01Sn/4Si) and Al/Si ratios (up to the value of 0.005Al/4Si) resulted in a magadiite structure. Synthesis methods applied to Sn-modified materials were found to be unsuitable for the introduction of tetrahedrally substituted Al. The characterization methods used were X-ray diffraction (XRD), temperature-programmed reduction (TPR), and diffuse reflectance infrared fourier transform (DRIFT) spectroscopy. and these indicated the presence of metal oxide species on the surfaces of the crystals, in addition to a small degree of replacement of Si by Sn or Al in the tetrahedral layers.

Key Words—H_2-TPR, Ilerite, Magadiite, Textural Properties, Tin Silicate, XRD.

INTRODUCTION

Si-based porous materials, *i.e.* zeolites or zeolite-like materials, have proven to be very successful catalysts, supports, or ion exchangers (Cejka and van Bekkum, 2005). One of the basic building blocks of their framework is the Si tetrahedron. Isomorphous substitution for Si by other atoms, *i.e.* Al, Ti, Sn (referred to here as heteroatoms), usually leads to materials with significantly different properties because of the additional acid/base or redox active sites created.

One of the best known examples of such modifications is titanosilicalite (TS-1), with isolated transition metal ions introduced into the tetrahedral framework positions (Wróblewska *et al.*, 2006). Titanosilicalite has proved to be an efficient catalyst for mild oxidation reactions; the small radii of its pores limit its application in the oxidation of bulky organic compounds significantly, however. As a result, material with similar properties to the three-dimensional silicates which can also be modified by means of isomorphous substitution in the silicate structure is needed.

One possible solution could be layered silicates (Figure 1). The silica layers consists of one (ilerite), two (magadiite), or three (kenyaite) tetrahedral sheets. In contrast to the well defined and well characterized three-dimensional structures, the structures of many of the two-dimensional silicates are still under discussion (Borowski *et al.*, 2008; Brenn *et al.*, 2000). The advantage compared with the microporous, three-dimensional structure of zeolites, is the option to adjust the

distance between the silica layers, thus enabling bulky organic molecules to access the active centers located in the layers and allowing their application in liquid-phase oxidation reactions.

Sodium silicates are typical examples of such layered materials, the synthesis of which was described by Bergk *et al.* (1987). They are distinguished by their great ion-exchange selectivity and capacity. The properties of Na-silicates can be adjusted relatively easily by ion exchange of interlayer cations. Ishii *et al.* (2009), after alkoxysilylation of ilerite with p-aminotrimethoxysilane, synthesized a microporous layered organic-inorganic hybrid. Guerra *et al.* (2010) described the ability of magadiite, modified with 5-mercapto-1-methyltetrazole (MTTZ), to remove Th(IV), U(VI), and Eu(III) from aqueus solution. After intercalation of acetic acid into ilerite, Ikeda *et al.* (2008) synthesized the siliceous zeolite RWR. The introduction of active compounds containing metals such as Pd, Ta, Pt, Ti, or Fe is also usually achieved by ion exchange (Ishimaru *et al.*, 2004; Kim *et al.*, 2001; Kuhlmann *et al.*, 2004; Kim *et al.*, 2006). Those modified materials were reported to be active in various reactions, *i.e.* vapor-phase Beckmann rearrangement of cyclohexanone oxime (Kim *et al.*, 2004) or conversion of n-hexane (Kuhlmann *et al.*, 2004).

A different approach to modify layered silicates was described by Borbély *et al.* (1991), Pál-Borbély *et al.* (1998), and Superti *et al.* (2007), which resulted in successful attempts at isomorphous substitution of Si by Al ions. Such materials were used as a precursor in the synthesis of zeolite (Pál-Borbély *et al.*, 1998). Superti *et al.* (2007) also pointed out the very interesting properties of such modified magadiites and their possible catalytic applications. This successful introduction of heteroatom substitution into silica layers suggests that the introduc-

* E-mail address of corresponding author:
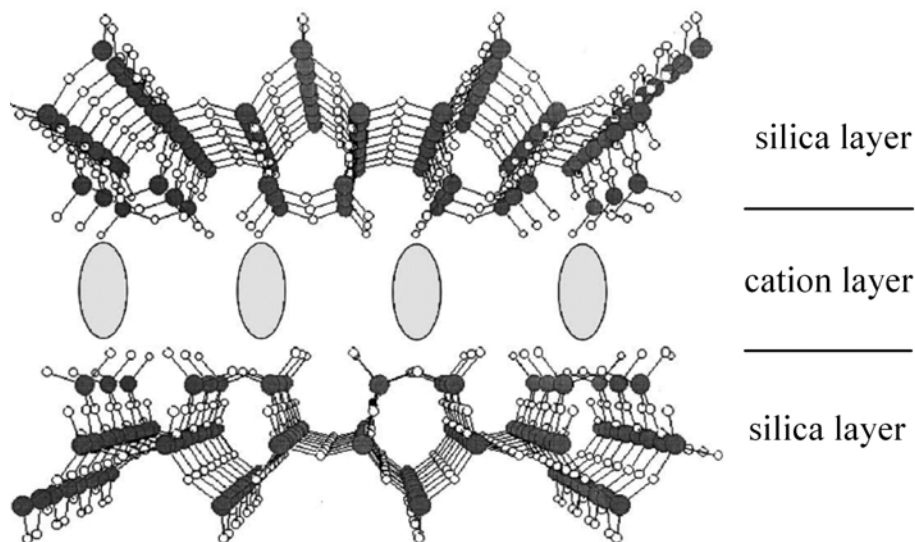wojciech_supronowicz@o2.pl

Figure 1. Proposed structural model of ilerite (Kim *et al.*, 2004).

tion of other transition metals may also be possible. Such materials could be used as efficient catalysts and a complete study of synthesis methods and their properties is required.

Corma *et al.* (2003) and Boronat *et al.* (2007) described microporous materials containing Sn as active catalysts in redox reactions, *e.g.* Meervein-Pendorv-Verley reduction or Baeyer-Villiger oxidations. Villa de P *et al.* (2005) described a Sn-pillared kenyaite as a material that is active in nopol synthesis (nopol is an optically active bicyclic primary alcohol, useful in the agrichemical industry for the synthesis of pesticides, soap fragrances, and household products). Sn-substituted layer silicates are, therefore, proposed as being potentially catalytically active in the reactions mentioned. Incorporation of Sn ions into silica layers could result in material which could be pillared later and used as a catalyst. The first step of such an investigation is, of course, an attempt to replace isomorphously some of the Si by Sn ions. The aim of the present work was to investigate the influence of the presence of a source of Sn, namely, $SnCl_4 \cdot 5H_2O$, on the synthesis of Sn-substituted layer silicates. Some syntheses in which Si was partially substituted by Al were also of interest for comparison purposes.

EXPERIMENTAL

The theoretical unit-cell formula for ilerite is xM:Na_2O:$(8-x)SiO_2$:$9H_2O$ (Borbély *et al.*, 1991), where M represents Sn or Al with $0 \leqslant x \leqslant 0.010$. For all syntheses, colloidal silica (CWK Bad Koestritz, Bad Koestritz, Germany) as the silica source and NaOH (Merck, Darmstadt, Germany) as the alkali source were used. Aluminum isopropoxide (Fluka, Seelze, Germany)

and Sn(IV) chloride pentahydrate (Riedel-de Haen, Seelze, Germany) were used as the sources of the heteroatoms. Synthesis procedure I, similar to that described by Borbély *et al.* (1991), consisted of mixing colloidal silica with deionized water for 15 min and then adding a mixture containing a heteroatom source and NaOH (Figure 2) dissolved in deionized water. After mixing, a dense gel was formed immediately (pH ≈ 14). The molar ratio of the reactants in the pre-synthesis mixture was xM:$4SiO_2$:$(yx+1)Na_2O$:$30H_2O$, where $y = 4$ or 6, $x \leqslant 0.010$, and M = Sn or Al, which is similar to that described in the work of Borbély *et al.* (1991). After 45 min of stirring, the gel was placed in a teflon-lined stainless steel autoclave. Crystallization took place at 373 K in static conditions over 3 or 4 weeks. The solid material synthesized was washed and dried at 323 K. The resulting samples were named according to heteroatom to silicon atom ratios in the synthesis mixture, *i.e.* xM/4Si, where M = Al or Sn and x is the molar ratio of M. The reference material was 1.27 wt.% SnO_2 added to Na-ilerite (denoted as SnO_2/Na-ilerite).

Procedure II was adapted from Kim *et al.* (2004) (Figure 2) and differed from procedure I in the time of mixing of the starting gel (24 h) and in the temperature and time used for crystallization (383 K, 10 days). The molar ratio of the reactants was the same as in procedure I.

In order to check the influence of crystallization time on the synthesis, samples crystallized for 15 days, at 383 K, were also synthesized. According to Iwasaki *et al.* (2006), some syntheses were modified by the use of seeds of ilerite (particularly in samples with $0.005 \leqslant x \leqslant 0.010$), with the intention of enhancing the yield of the synthesis.

All samples were modified by ion exchange in order to obtain their H-forms. Two g of sample was added to
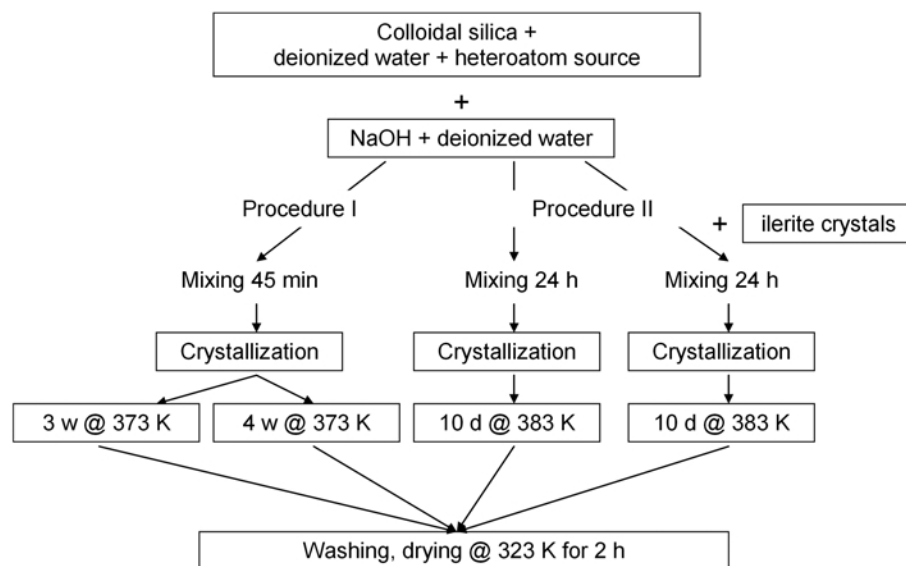
Figure 2. Different synthesis procedures: w − weeks, d − days.

40 mL of deionized water. The pH was adjusted to pH 2 by adding 0.1 M HCl. After 24 h of stirring, the H form of the material was washed, filtered, and dried at 323 K for 2 h.

X-ray diffraction (XRD) patterns were recorded using a Stoe STADI P (Darmstadt, Germany) instrument. Scanning electron microscopy (SEM) images were taken using a FEI QUANTA 200 3D microscope (Eindhoven, The Netherlands).

The N_2 adsorption isotherms were obtained using an Autosorb-1 Quantachrome surface area analyzer. Prior to N_2 adsorption, the samples were evacuated at 573 K and the BET method was used to calculate the surface area, porosity, and pore diameter. Pore-size distribution was determined using the Density Functional Theory (DFT) method (Lowell et al., 2004).

Inductively coupled plasma atomic emission spectroscopy (ICP-AES) analysis was carried out with a Thermo Scientific iCAP 6000 series instrument using a 100 mg sample dissolved in 500 mg of 48% HF solution.

In differential thermal analysis and thermal gravimetry analysis (DTA/TG) measurements, samples were heated to 1273 K (10 K/min) in an N_2 atmosphere.

In the hydrogen temperature-programmed reduction (H_2-TPR) analysis (Raczek Analysentechnik), 0.2 g of sample (fraction 315−200 μm) was placed in a quartz u-tube. During pretreatment the sample was heated to 573 K (with a heating rate of 25 K/min) in an Ar atmosphere (50 mL/min), held for 2 h, and then cooled to 373 K. The reduction measurement was then conducted in a flowing Ar + 7.5% H_2 atmosphere (50 mL/min) by heating the samples to 973 K (5 K/min). Hydrogen consumption was detected by a thermal conductivity (TCD) detector.

DRIFT spectra were recorded at 373 K under an N_2 purge (flowing at 50 mL/min) using a Bruker EQIUNOX 55 FTIR spectrometer equipped with a diffuse reflectance cell. Samples were prepared as KBr discs (sample:KBr = 1:5).

RESULTS AND DISCUSSION

The XRD patterns of the samples synthesized (Figures 3−6) revealed patterns from synthesis procedures I and II that were consistent with the formation of ilerite, according to Vortmann et al. (1997) who reported diffraction peaks at ~8, 18.6, 21.8, 25.6, and 29.2º2θ as being typical for ilerite structures. The presence of additional diffraction peaks after prolonging the time of the synthesis, especially that at 5.75º2θ, indicated traces of a magadiite-phase impurity.

The addition of Sn to the pre-synthesis mixture resulted in the formation of magadiite instead of ilerite, as indicated by characteristic diffraction peaks at ~5.75, 17.10, 26.00, 27.00, and 28.00º2θ (Feng et al., 2003). Samples with Sn content greater than a molar ratio of 0.002 were amorphous; however, with greater Sn loading (0.003 ⩽ Sn ⩽ 0.005), adding amounts of additional NaOH to supplement the amount of alkalinity needed for in situ formation of sodium hexahydroxo stannate (IV) from Sn(IV) chloride pentahydrate during synthesis also resulted in the formation of magadiite (Figure 4). When Al (alumina isopropoxide) was added to the synthesis procedure, however, magadiite did not form. Only the sample with the smallest Al content (Figure 5a) was crystalline. In synthesis mixtures for samples with 0.003 ⩽ Al ⩽ 0.010 and Sn >0.005, no crystallization products were found after 10 days. The
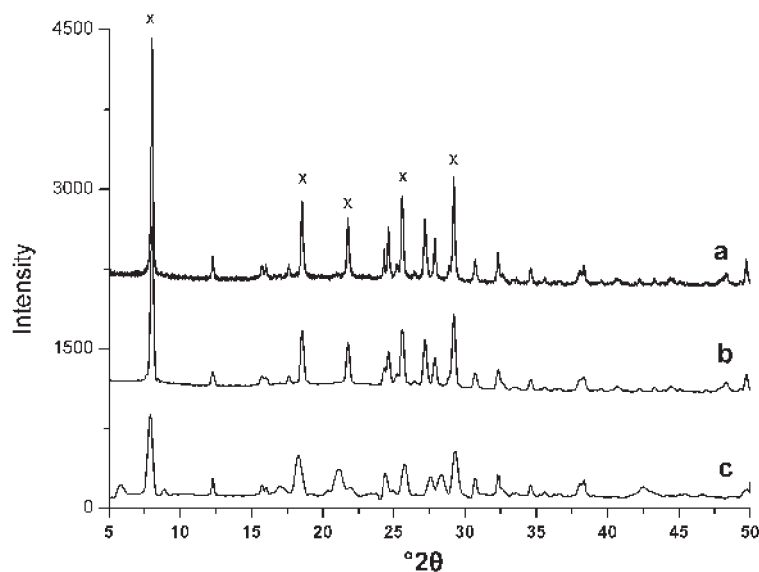
Figure 3. XRD patterns of Na-forms of: (a) ilerite − procedure II; (b) ilerite − procedure I − 3 weeks; (c) ilerite − procedure I − 4 weeks.

crystallization time in procedure II was, therefore, prolonged to 15 days to test the influence of the crystallization time. Tin-containing samples obtained by this modified method were found to contain large amounts of amorphous material (significant increase in the baseline, Figure 6b) and some magadiite. In the case of Al-modified samples (Figure 5c), the magadiite structure was detected for samples with ratios of 0.005Al/4Si. However, the addition of larger amounts of Al to the synthesis gel again resulted in the formation of an amorphous phase.

Synthesis of crystalline samples with compositions of 0.010Sn/4Si was possible only after seeding the pre-synthesis mixture with ilerite. As in the case described above, for greater Sn substitution, the seeding method yielded magadiite as the dominant layer silicate phase. However, a low intensity of peaks and a high background indicate a low degree of crystallinity and the presence of impurities as amorphous phases (Figure 6a). An increase in the crystallization time to 15 days led to the formation of a significant amount of quartz (Figure 6b), as indicated by the diffraction peak at 13.8º2θ.
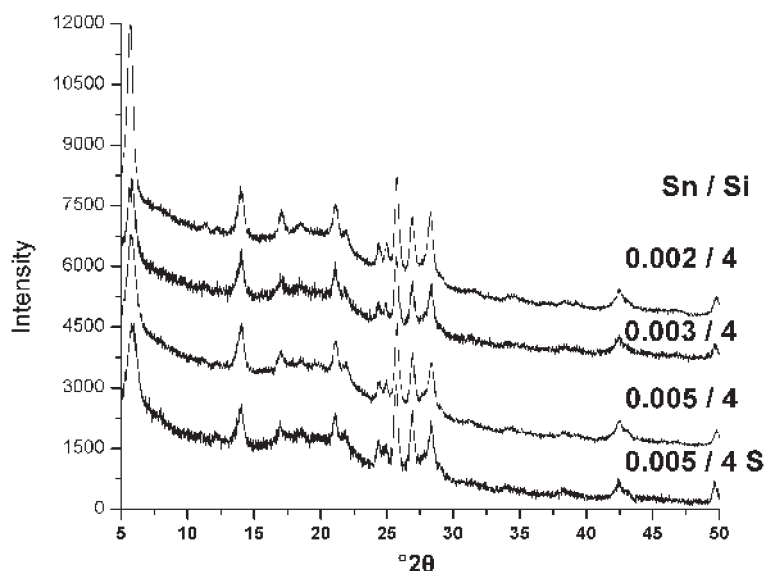

Figure 4. XRD patterns of various Na-forms of Sn-containing samples synthesized according to procedure II with additional alkali. S − synthesis in the presence of ilerite seeds.
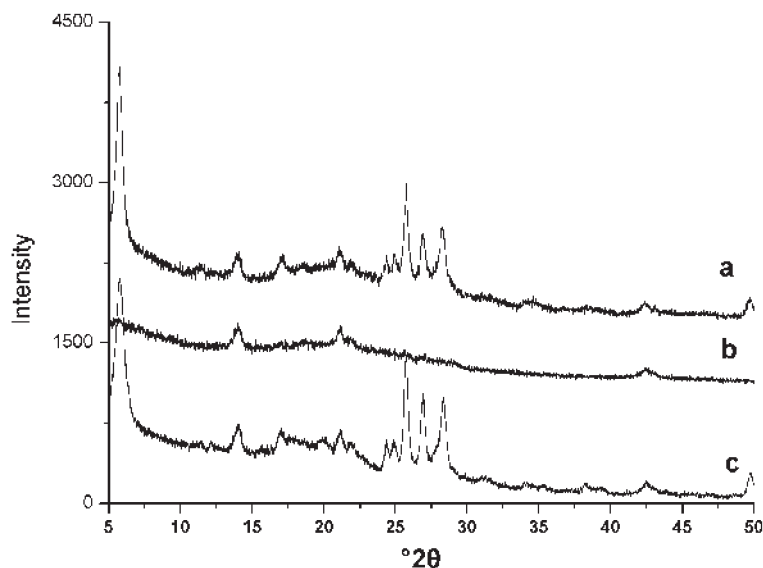
Figure 5. XRD patterns of Na-forms of: (a) 0.002Al/4Si magadiite − procedure II (10 days, 383 K); (b) 0.005Al/4Si magadiite − procedure II (10 days, 383 K); (c) 0.005Al/4Si magadiite − procedure II (15 days, 383 K, additional alkali).

A similar influence of crystallization time was observed in the case of 0.01Al/4Si samples (Figure 6c,d). Furthermore, the intense peak at 33.7°2θ indicated the presence of a Na_2CO_3 phase (Swainson *et al.*, 1995), probably occluded in amorphous silica. After 15 days of crystallization, mordenite (Chandwadkar *et al.*, 1991; Meier, 1961) dominated the sample.

Incorporation of heteroatoms into silica layers leads to crystallographic stress or defects due to differences in cationic radii. Theoretically, substitution for Si should cause less stress in material with only one silica layer, *i.e.* ilerite, thus, a greater stability for the heteroatom-modified ilerite can be expected. Conversely, a small Sn content in the resulting products and the dominance of the magadiite phase in the modified samples indicate that the second silica layer may have a significant influence on the stability of the modified structure.

The SEM images in Figures 8 and 9 indicated that all modified samples consisted of irregular, plate-shaped crystals and agglomerates which are atypical for either
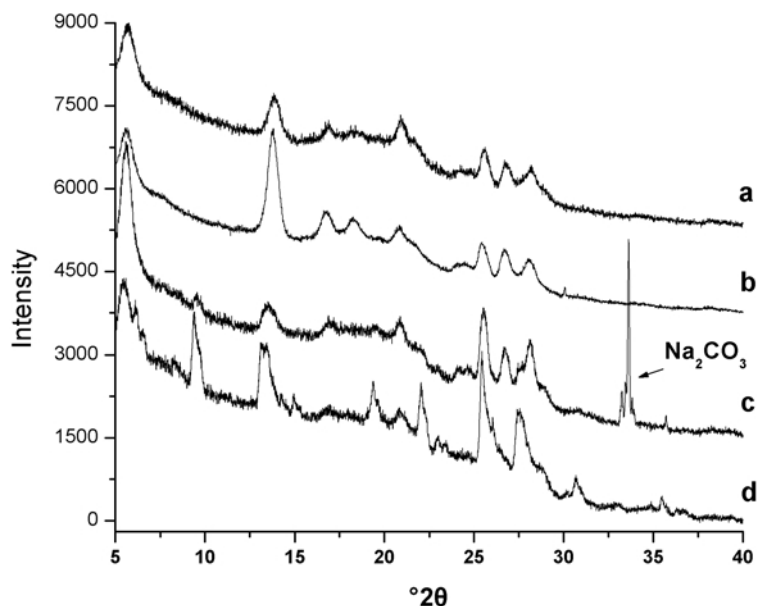

Figure 6. XRD patterns of Na-forms of samples synthesized according to procedure II with additional alkali and the addition of ilerite seeds to the initial mixture: (a) 0.01Sn/4Si − 10 days; (b) 0.01Sn/4Si − 15 days; (c) 0.01Al/4Si − 10 days; (d) 0.01Al/4Si − 15 days .

ilerite or magadiite phases. Small amounts of rosette-shaped crystals (Iwasaki *et al.*, 2006) confirmed the existence of magadiite. Considering the XRD data (Figures 4−6), one can assume that in synthesized samples, magadiite crystals do exist as a massive structure, as found in nature (Sebag *et al.*, 2001). Neither the pathway for the synthesis nor the heteroatom loading significantly affected the crystal shape (Figure 8). Furthermore, the morphology of crystals (Figure 9) was unchanged after the ion exchange of Na ions by protons.

The presence of Sn in the samples was confirmed by ICP-AES elemental analysis (Table 1). The observed values, which are the sum of Sn from all Sn species present in the material, correlated well with the amount of Sn in the synthesis mixture. The largest amount of Sn was detected in samples synthesized in the presence of ilerite seeds. The amounts of Sn were much smaller than the amount of Al reported for Al-modified magadiite (Pál-Borbély *et al.*, 1998).

The DTA/TG studies were carried out in order to establish the thermal properties of the reaction products. The patterns for synthetic ilerite (Figure 10) correspond well with those described by Borbély *et al.* (1991). Endothermic peaks at ~400 K and 450 K (Figure 10) were attributed to the desorption of water from the interlayer space and the removal of the hydration shell of Na^+ cations, respectively. The slow decrease in weight at temperatures >500 K was due to dehydroxylation of the ilerite and recrystallization occurred at ~750 K. Sample pretreatment was, therefore, carried out below this temperature.

The amount of water desorbed did not change significantly with increasing heteroatom loading. This indicated the absence of Sn as a free cation between the layers. Furthermore, no clear influence of the synthesis method on the thermal behavior was found. Shifts in the DTA/TG profiles were within the range of accuracy of the measurement equipment (Figure 11).
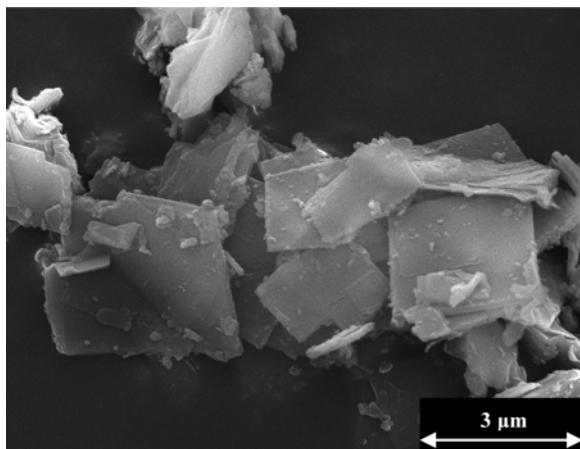

Figure 7. SEM image of unmodified Na-ilerite (procedure II).

Table 1. Sn/Si ratio in synthesis mixtures and Sn content in bulk solid, determined by ICP-AES.

Sn/Si in synthesis mixture	Sn/Si in sample
0.00050	0.00027
0.00075	0.00064
0.00125	0.00090
0.00125 S	0.00112 S

S − synthesis in the presence of ilerite seeds.

Unlike the DTA profile of the Na-form, the H-exchanged forms contained only one desorption peak (Figure 12). This allows one to assume that the desorption maximum at 447 K, in the profile of Na-ilerite (Figure 10), can be assigned to the desorption of water from the hydration shell of the Na ion. As stated above, the exchange of Na by protons was nearly complete.

The N_2 adsorption isotherm of the investigated samples (Figure 13) belongs to type III in the IUPAC nomenclature. After considering its shape and calculated pore-size distribution (Figure 14), as well as the XRD profiles (Figures 4−6), the presence of micropores >20 Å in size can be excluded. On the other hand, adsorption/desorption hysteresis indicated the presence of mesopores and macropores. Large basal spacings were, however, absent from the XRD patterns of the synthesized samples, indicating that the structure does not exhibit such large basal spacings and the condensation of N_2 was evidently in the inter-particle space (see also Figures 7−9). The isotherms of other samples were similar (data not shown). The surface areas of the

Table 2. BET surface area for various samples synthesized according to procedure II with additional alkali.

Sn/Si	Surface area (m^2/g)
0 Sn/4 Si	100
H − 0 Sn/4 Si	53
0.005 Sn/4 Si	103
H − 0.005 Sn/4 Si	100
0.005 Sn/4 Si S	107
H − 0.005 Sn/4 Si S	106
0.010 Sn/4 Si S	32
H − 0.010 Sn/4 Si S	34
SnO_2 impregnated on ilerite	30

Al/Si	Surface area (m^2/g)
0.005 Al/4 Si *	109
H − 0.005 Al/4 Si *	112

* synthesis in 15 days, S − synthesis in the presence of ilerite seeds.

synthesized samples (Table 2) were unaffected by increasing Sn content, as the Sn-loading was very small (up to 0.112 wt.%). Only in the case of the sample with the largest Sn loading did the surface area decrease significantly (Table 2), revealing a value similar to that of ilerite impregnated with SnO_2. This suggests that bulky Sn oxide, as well as amorphous material, were present on the surface of the material (0.010Sn/4Si). The surface area of the material was not significantly changed after ion exchange.

Recorded DRIFT spectra in the range of lattice vibrations (Figure 15) for Na-ilerite were similar to those described by Kim *et al.* (2004) and Borbély *et al.* (1991). On the other hand, spectra from samples with the smallest and medium levels of Sn loading (with magadiite structure) (Figure 15d), synthesized by seeding with ilerite, and which yielded a large amount of Sn in the material, contained an additional band at 970 cm^{-1}. This band can contribute to the *Me*−O−Si stretching band (Kim *et al.*, 2004; Borbély *et al.*, 1991) and may indicate the presence of a heteroatom in layers or pillars of Sn-containing compounds bound to the layer surface. However, such a band is not unique because it can also be ascribed to Si−O−H vibrations which occur
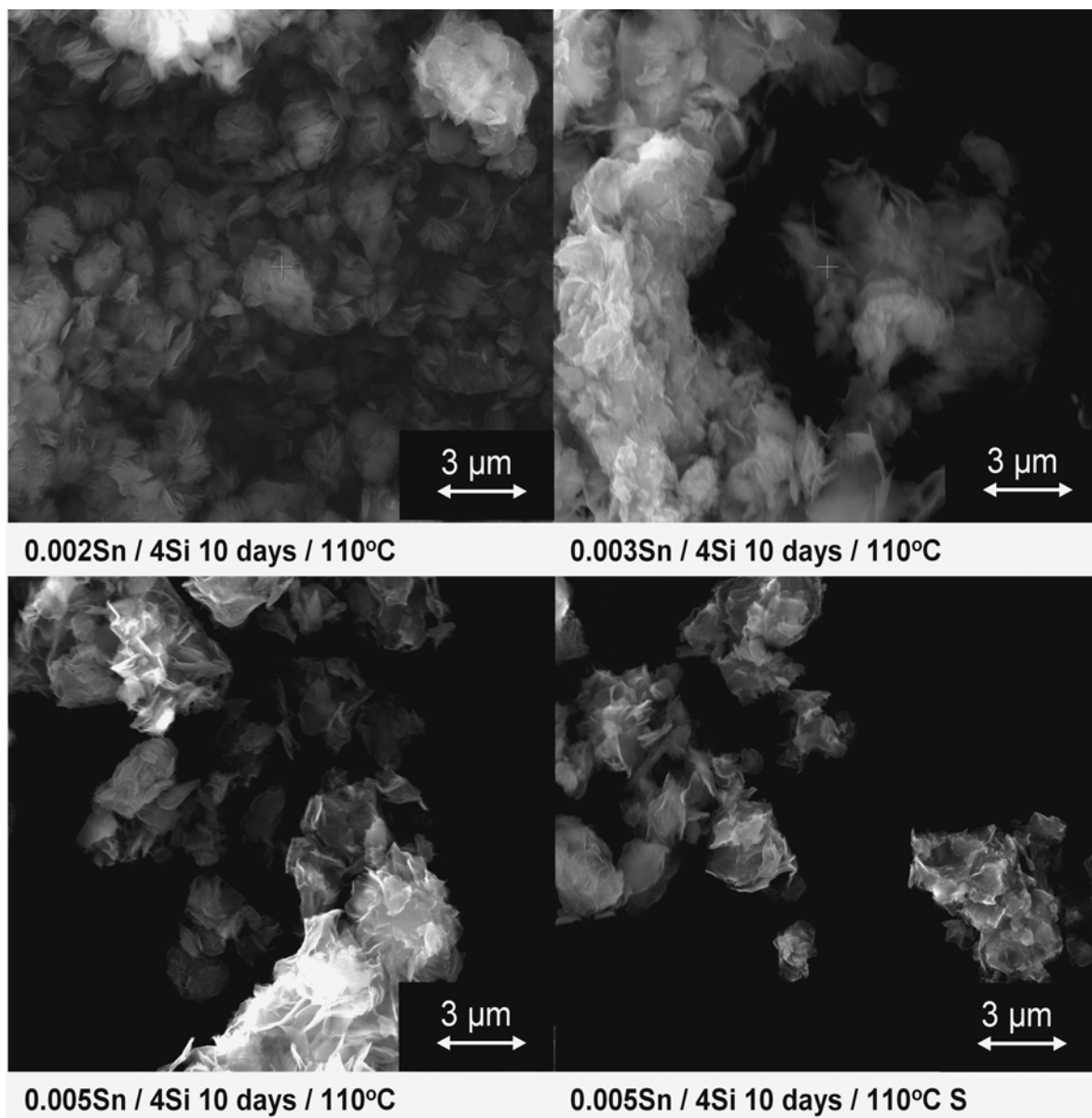

Figure 8. SEM images of various Na-forms of Sn-containing samples (procedure II with additional alkali). S − synthesis in the presence of ilerite seeds.
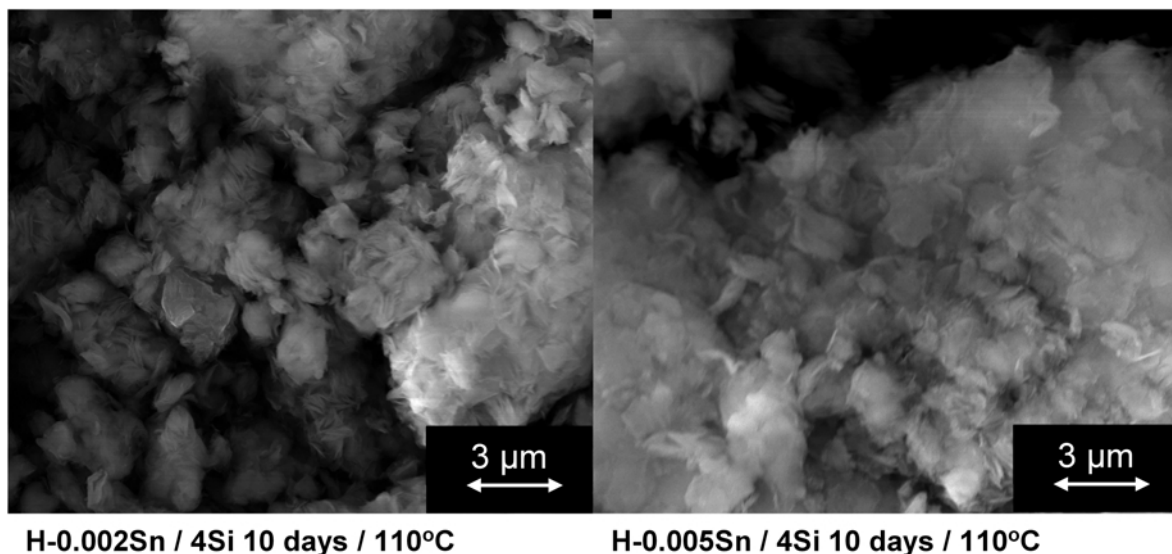
H-0.002Sn / 4Si 10 days / 110°C   H-0.005Sn / 4Si 10 days / 110°C

Figure 9. SEM images of various H-forms of Sn-containing samples (procedure II with additional alkali).

at 977 cm^{-1} in H-ilerite. All H-forms of Sn- or Al-substituted samples showed a similar band; thus, the assignment to a Si−O−H vibration seems more likely. Additionally, in unmodified H-ilerite and in Al-containing H-ilerite, a band at 920 cm^{-1} was detected, which also can contribute to Si−O−H vibrations.

The redox properties of Sn in modified samples were investigated by H_2-TPR (Figure 16). Under the conditions that were applied, bulky SnO_2 (Figure 16) was reduced to Sn(0) at ~890 K in a one-step reduction (Auroux *et al.*, 2000; Haneda *et al.*, 2001; Janiszewska *et al.*, 2009). On the other hand, others (Auroux *et al.*; Lazar *et al.*, 2000; Janiszewska *et al.*, 2009) have reported that reduction of supported SnO_2 occurs in a two-step reduction, from Sn(IV) to Sn(II) and from Sn(II) to metallic Sn. As confirmed by Lazar *et al.* (2000), the nature of the support has a significant influence on the temperature and reduction steps of SnO_2. In order to investigate the influence of support on the reduction of SnO_2, Na-ilerite impregnated with Sn oxide was tested. Compared to Na-ilerite (Figure 16), two additional peaks were recorded at ~675 K and ~820 K. The amount of H_2 consumed was calculated, and found to be equal for both peaks; and the amount of hydrogen required to reduce Sn in the investigated material was comparable. This seems to confirm the two-step reduction mechanism of supported SnO_2.

Note that due to the small amount of reducible species, the TPR profiles were close to the detection
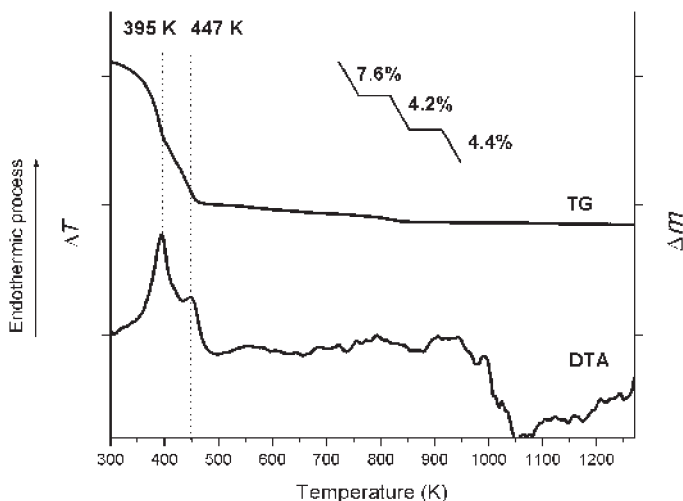

Figure 10. DTA/TG profile of unmodified Na-ilerite. Mass loss percentage is given in the upper part of the graph.
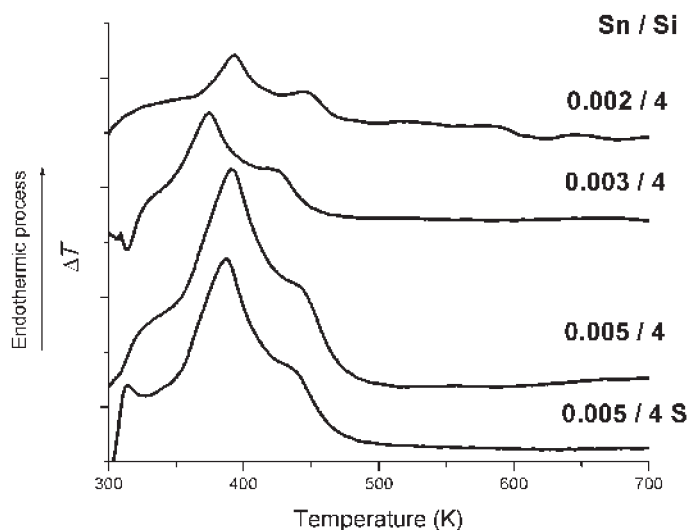
Figure 11. DTA profiles of various Na-forms of Sn-containing samples synthesized according to procedure II with additional alkali. S − synthesis with ilerite seeds. The data were not normalized relative to sample amount.

limit of the method. The baseline was, therefore, strongly influenced by the background noise and the baking of the sample, as represented by the peak at ~625 K (Figure 16, sample Na-ilerite). This effect was absent from the quartz samples.

Tin-containing samples exhibited a peak at ~525 K (Figure 16), which was attributed to the reduction of small Sn oxide particles well dispersed between silica layers.

The stabilization effect of the silica layer clearly invoked a higher temperature for the reduction of the Sn incorporated. Therefore, small additional peaks (Figure 16) at ~725 K and ~815−850 K were assigned to the reduction of Sn that was present in the tetrahedral layers. Because the change of the baseline caused by the change in the hydrodynamic conditions due to the baking of the sample could not be separated, quantitative
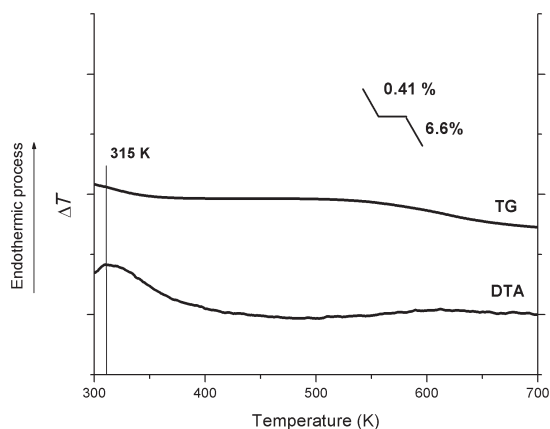

Figure 13. Isotherm of N_2 adsorption of 0.005Sn/4Si sample − procedure II with additional alkali.

Figure 12. DTA/TG profile of the H form of 0.005Sn/4Si − 10 days of synthesis with ilerite seeds. Mass loss percentage is given in the upper part of the graph.
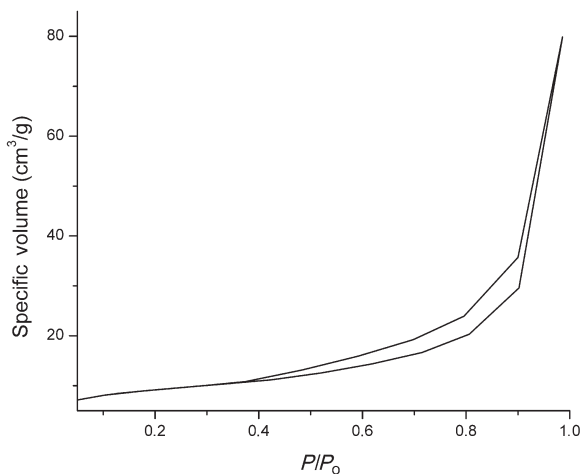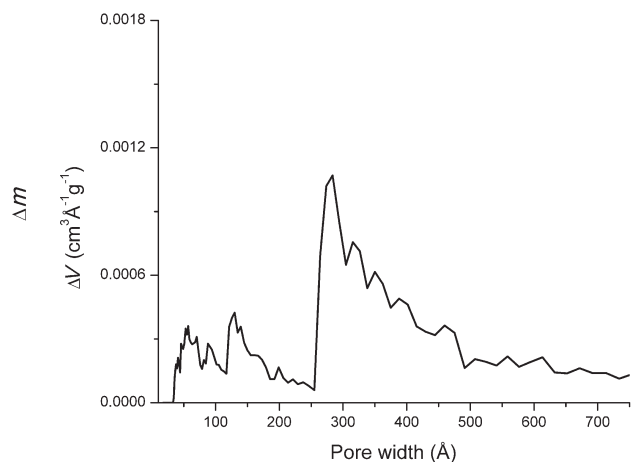

Figure 14. Pore-size distribution for 0.005Sn/4Si sample − procedure II with additional alkali.
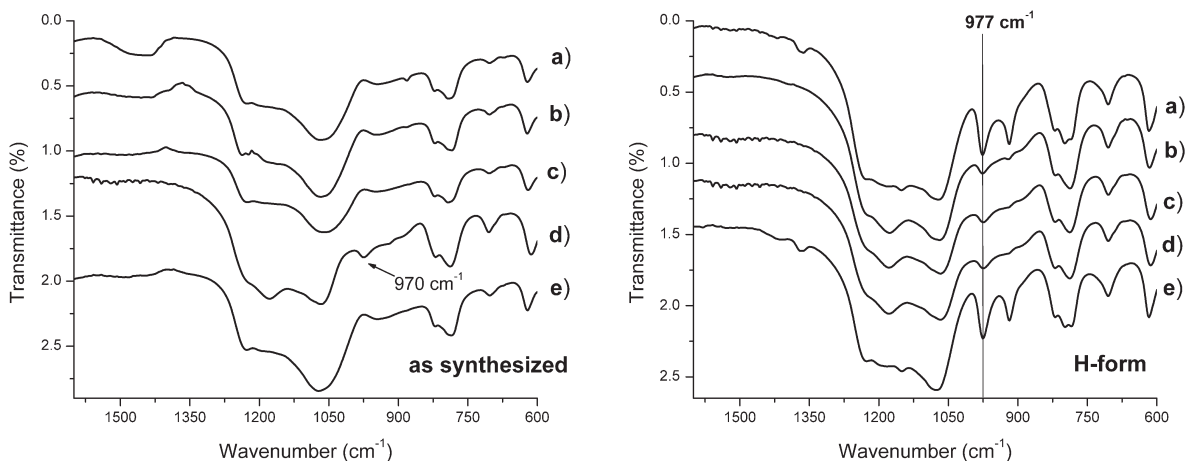
Figure 15. DRIFT spectra of various Sn- or Al-containing samples synthesized according to procedure II. To the left − as synthesized, to the right − H-forms: (a) unmodified ilerite; (b) 0.003Sn/4 Si; (c) 0.005Sn/4 Si; (d) 0.005Sn/4 Si − 10 day synthesis with ilerite seeds; (e) 0.005Al/4 Si − 15 day synthesis.

analysis giving the distribution of Sn between interlayer and tetrahedral sites was impossible.

CONCLUSIONS

Na-ilerite was synthesized successfully under hydrothermal conditions. The addition of a small amount of aluminum isopropoxide or Sn(IV) chloride pentahydrate directed the synthesis to the magadiite structure. The crystallization process was shown to be strongly influenced by the amount of OH^- and Na^+ ions.

The presence of only one silica layer seems to have significant influence on the stability of the layer silicate; therefore, modified materials were found to have the structure of magadiite, which is more stable due to the second silica tetrahedral layer. The use of ilerite seeds in the synthesis enhances both the number of crystallites and the total Sn loading in the material. Nevertheless, despite the presence of ilerite seeds, synthesis led to the more stable structure, magadiite.

The synthesis method used to prepare Sn-modified samples was not suitable, however, for the introduction of tetrahedral Al. Prolongation of the synthesis time failed to produce a layered structure with Al content >0.002Al/4Si.

H_2-TPR appeared to indicate the presence of a small number of metal oxide pillars between the silica layers, in addition to a small degree of substitution of Sn for Si in the tetrahedral layers.

REFERENCES

Auroux, A., Sprinceana, D., and Gervasini, A. (2000) Support effects on de-NOx catalytic properties of supported tin oxides. *Journal of Catalysis*, **195**, 140−150.

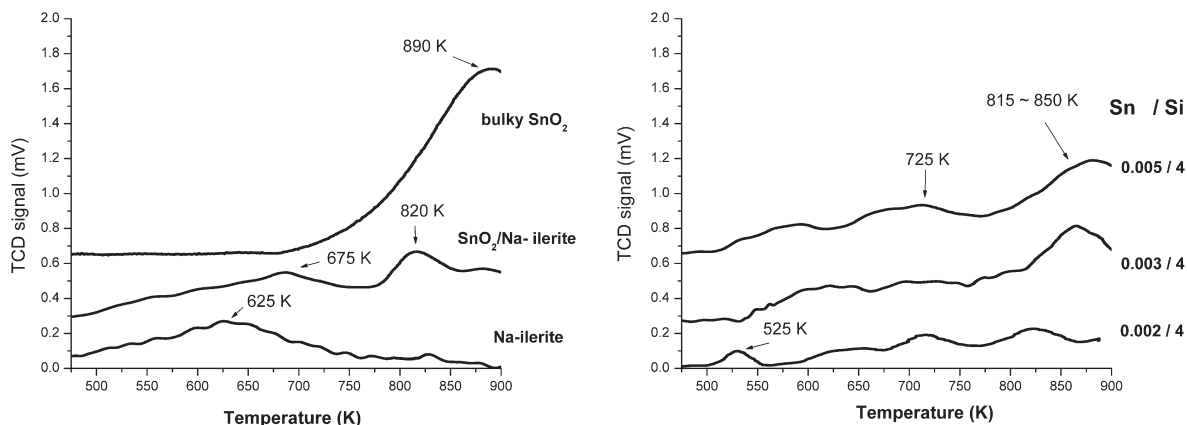Bergk, K.-H, Schwieger, W., and Porsch, M. (1987)

Figure 16. H_2-TPR profiles of various samples. Na-ilerite sample was synthesized according to procedure II. Sn-containing samples were synthesized according to procedure II with additional alkali.

Aluminiumfreie Schichtsilicathydrate − Synthese und Eigenschafts-Anwendungs − Beziehungen, Teil II. *ChemTech*, **11**, 459−504

Borbély, G., Beyer, H.K., Karge, H.G., Schwieger, W., Brandt, A., and Bergk, K.H. (1991) Chemical characterization, structural features, and thermal behavior of sodium and hydrogen octosilicate. *Clays and Clay Minerals*, **39**, 490−497.

Boronat, M., Concepcion, P., Corma, A., and Renz, M. (2007) Peculiarities of Sn-Beta and potential industrial applications. *Catalysis Today*, **121**, 39−44.

Borowski, M., Kovalev, O., and Gies, F. (2008) Structural characterization of the hydrous layer silicate Na-RUB-18, $Na_8Si_{32}O_{64}(OH)_8 \cdot 32H_2O$ and derivatives with XPD-, NPD-, and SS NMR experiments. *Microporous and Mesoporous Materials*, **107**, 71−80.

Brenn, U., Ernst, H., Freude, D., Herrmann, R., Jaehning, R., Karge, H.G., Kaerger, J., Koenig, T., Maedler, B., Pingel, U.-T., Prochnow, D., and Schwieger, W. (2000) Synthesis and characterization of the layered sodium silicate, ilerite. *Microporous and Mesoporous Materials*, **40**, 43−52.

Cejka, J. and van Bekkum, H. (editors) (2005) Zeolites and Ordered Mesoporous Materials: Progress and Prospects. *Studies in Surface Science and Catalysis*, **157**, 380 pp., Elsevier, Amsterdam.

Chandwadkar, A., Bhat, R., and Ratnasamy, P. (1991) Synthesis of iron-silicate analogs of zeolite mordenite. *Zeolites*, **11**, 42−47.

Corma, A., Domine, M.E., and Valencia, S. (2003) Water-resistant solid Lewis acid catalysts: Meerwein-Ponndorf-Verley and Oppenauer reactions catalyzed by tin-beta zeolite. *Journal of Catalysis*, **215**, 294−304.

Feng, F. and Balkus, K.J. (2003) Synthesis of kenyaite, magadiite and octosilicate using poly(ethylene glycol) as a template. *Journal of Porous Materials*, **10**, 5−15.

Guerra, D.L., Ferrreira, J.N., Pereira, M.J., Viana, R.R., and Airoldi, C. (2010) Use of natural and modified magadiite as adsorbents to remove Th(IV), U(VI), and Eu(III) from aqueous media − thermodynamic and equilibrium study. *Clays and Clay Minerals*, **58**, 327−339.

Haneda, M., Ohzu, S., Kintaichi, Y., Shimizu, K., Shibata, J., Yoshida, H., and Hamada, H. (2001) Sol-gel prepared Sn-Al_2O_3 catalysts for the selective reduction of NO with propene. *Bulletin of the Chemical Society of Japan*, **74**, 2075−2081.

Ikeda, T., Oumi, Y., Takeoka, T., Yokoyama, T., Sano, T., and Hanaoka, T. (2008) Preparation and crystal structure of RUB-18 modified for synthesis of zeolite RWR by topotactic conversion. *Microporous and Mesoporous Materials*, **110**, 488−500.

Ishii, R., Ikeda, T., and Mizukami, F., (2009) Preparation of a microporous layered organic-inorganic hybrid nanocomposite using p-aminotrimethoxysilane and a crystalline layered silicate, ilerite. *Journal of Colloid and Interface Science*, **331**, 417−424.

Ishimaru, S., Togawa, M., Shinohara, E., Ikeda, R., Kawasaki, H., and Maeda, H. (2004) Structures and dynamics of dodecyldimethylamine oxide intercalated into RUB-18. *Journal of Physics and Chemistry of Solids*, **65**, 425−427.

Iwasaki, T., Kuroda, T., Ichio, S., Satoh, M., and Fujita, T. (2006) Seeding effect on crystal growth in hydrothermal synthesis of layered octosilicate. *Chemical Engineering Communications*, **193**, 69−76.

Janiszewska, E., Kowalak, S., Supronowicz, W., and Roessner, F. (2009) Synthesis and properties of stannosilicates. *Microporous and Mesoporous Materials*, **117**, 423−430.

Kim, M.H., Ko, Y., Kim, S.J., and Uh, Y.S. (2001) Vapor phase Beckmann rearrangement of cyclohexanone oxime over metal pillared ilerite. *Applied Catalysis, A: General*, **210**, 345−353.

Kim, S.J., Jung, K.-D., Joo, O.-S., Kim, E.J., and Kang, T.B. (2004) Catalytic performance of metal oxide-loaded Ta-ilerite for vapor phase Beckmann rearrangement of cyclohexanone oxime. *Applied Catalysis, A: General*, **266**, 173−180.

Kim, S.J., Kim, E.J., Kang, T.B., Jung, K.-D., Joo, O.-S., and Shin, C.-H., (2006) Synthesis and characterization of transition metal oxide-pillared materials with mesoporosity from layered silicate ilerite. *Journal of Porous Materials*, **13**, 27−35.

Kuhlmann, A., Roessner, F., Schwieger, W., and Gravenhorst, O. (2004) New bifunctional catalyst based on Pt containing layered silicate Na-ilerite. *Catalysis Today*, **97**, 303−306.

Lazar, K., Chandwadkar, A.J., Fejes, P., Cejka, J., and Ramaswamy, A.V. (2000) Valency changes of iron and tin in framework-substituted molecular sieves investigated by *in situ* Mössbauer spectroscopy. *Journal of Radioanalytical and Nuclear Chemistry*, **246**, 143−148.

Lowell, S., Shields, J.E., Thomas, M.A., and Thommes, M. (2004) *Characterization of Porous Materials and Powders: Surface Area, Pore Size and Density*. Springer, Dordrecht, The Netherlands.

Meier, W.M. (1961) The crystal structure of mordenite (ptilolite). *Zeitschrift für Kristallographie*, **115**, 439−450.

Pál-Borbély, G., Beyer, H.K., Kiyozumi, Y., and Mizukami, F. (1998) Synthesis and characterization of a ferrierite made by recrystallization of an aluminium-containing hydrated magadiite. *Microporous and Mesoporous Materials*, **22**, 57−68.

Sebag, D., Verrecchia, E.P., Lee, S.-J., and Durand, A. (2001) The natural hydrous sodium silicates from the northern bank of Lake Chad: occurrence, petrology and genesis. *Sedimentary Geology*, **139**, 15−31

Superti, G.B., Oliveira, E.C., Pastore, H.O., Bordo, A., Bisio, C., and Marchese, L. (2007) Aluminum magadiite: an acid solid layered material. *Chemistry of Materials*, **19**, 4300−4315.

Swainson, I.P., Dove, M.T., and Harris, M.J. (1995) Neutron powder diffraction study of the ferroelastic phase transition in sodium carbonate. *Journal of Physics: Condensed Matter*, **7**, 4395−4417.

Villa de P, A.L., Alarcón, E., and Montes de C, C. (2005) Nopol synthesis over Sn-MCM-41 and Sn-kenyaite catalysts. *Catalysis Today*, **107−108**, 942−948.

Vortmann, S., Rius, J., Siegmann, S., and Gies, H. (1997) *Ab initio* structure solution from X-ray powder data at moderate resolution: crystal structure of a microporous layer silicate. *Journal of Physical Chemistry B*, **101**, 1292−1297.

Wróblewska, A., Ławro, E., and Milchert, E. (2006) Technological parameter optimization for epoxidation of methallyl alcohol by hydrogen peroxide over TS-1 catalyst. *Industrial and Engineering Chemistry Research*, **45**, 7365−7373.